LARGE EDDY SIMULATIONS OF NON-EQUILIBRIUM PULSED TURBULENT FLOWS USING TRANSPORT EQUATIONS SUBGRID SCALE MODEL

Anne Dejoan *
Laboratoire IRPHE CNRS / Universités d'Aix-Marseille I & II
Technopôle de Château Gombert, BP 146 – 13384 Marseille Cedex 13, France
dejoan@icmcb.u-bordeaux.fr

Roland Schiestel
Laboratoire IRPHE CNRS / Universités d'Aix-Marseille I & II
Technopôle de Château Gombert, BP 146 – 13384 Marseille Cedex 13, France
Roland.Schiestel @irphe.univ-mrs.fr

ABSTRACT
A new two-equations subgrid-scale model is proposed for large eddy simulations using coarse grids. The characteristic subgrid-scale of turbulence is no longer given by the step size but is obtained by a dissipation equation. Thus, the model is better suited for non-equilibrium turbulence. The application to turbulence submitted to periodic forcing in pulsed channel flow shows some potentials of the method.

INTRODUCTION
Between the two extreme limits that are the DNS involving no modeling at all and the full statistical modeling in which the whole spectrum is modeled, lies the LES and VLES hybrid methods in which only the fine scale part of the energy spectrum is modeled while the large scale part is explicitly calculated. An important reduction of storage and computing time is then possible. Many subgrid scale models have been proposed in the scientific literature after the first proposal of Smagorinsky which is based on an implicit equilibrium hypothesis. Subgrid scale transport equations have been used in LES early by Deardorff (1973) and afterwards by Schumann (1975) and Horiuti & Yoshizawa (1986). But in all cases the characteristic length scale was given by the mesh cell size.

However, when the mesh is coarse and that the filter cutoff occurs at a wavenumber below the inertial range, the filter width is no longer a good estimate of the characteristic subgrid-scale turbulence length scale. The method proposed here is to introduce an ε-equation for calculating the length scale. This technique thus allows a consistent adaptation of statistical transport modeling transposed to subgrid scale closures.

The domain of applications is the LES or VLES method using coarse grids applied to turbulent flows undergoing non-equilibrium changes such as produced by unsteadiness in the mean or strong spatial variations. The application to unsteady turbulence submitted to periodic forcing illustrates the potentials of the method. Indeed, experimental results in pulsed channel flow (Binder and Kueny, 1981) have shown that lag effects occur between the various turbulence correlations and the mean flow. These properties are analyzed using phase averages that exhibit the non-equilibrium behavior of the turbulence field.

FILTERED EQUATIONS
The explicit filtered LES motion is governed by the following equations :

$$\frac{\partial \bar{U}_i}{\partial t}+\left(\overline{\bar{U}_i\bar{U}_j}\right)_{,j}=F_i-\frac{1}{\rho}\bar{\pi}_{,i}-\tau_{ij,j}+\nu\bar{U}_{i,jj} \quad (1)$$

$$\bar{U}_{i,i}=0 \quad (2)$$

The subgrid turbulent stresses are modeled by :

$$\tau_{ij}=-2\nu_{sgs}\bar{S}_{ij} \text{ with } S_{ij}=0.5(\bar{U}_{i,j}+\bar{U}_{j,i}) \quad (3)$$

The filtered Navier-Stokes equations are solved using an hybrid Adams-Bashforth and Crank-Nicolson time scheme and the space discretization is based on Hermitian fourth order schemes in the inhomogeneous directions and Fourier pseudo-spectral developments in the homogeneous directions (Schiestel and Viazzo, 1995).

* Present address : ICMCB, Univ. de Bordeaux, 86 av. du Dr. A. Schweitzer, 33608 Pessac, France

TRANSPORT EQUATIONS SUBGRID-SCALE MODEL

The model for homogeneous turbulence is based on integration in spectral space. The subgrid scale eddy viscosity $\nu_{sgs} = \mathcal{L}\sqrt{k_{sgs}}$ is based on the characteristic length scale $\mathcal{L}$ derived from a new ε-equation and k_{sgs} is given by its modeled transport equation. However the method can be easily applied to more general models such as non-linear models.

The subgrid-scale model behaviour has to be dependent of the location of the cutoff produced by the filter which lies between the two extreme limits that are the complete direct numerical simulation (DNS), and the one point full statistical modeling.

In coarse meshes, the spectral cutoff may be located before the inertial spectral range and the calculation is then a VLES (very large eddy simulation). If, in addition, the turbulence field is out of equilibrium, the step size of the mesh will no longer be a correct estimate of the characteristic turbulence length scale. A different method is proposed here in which subgrid-scale transport equations are introduced to derive the length scale. The typical field of application of the proposed method is non-equilibrium turbulence.

The ε-equation by spectral splitting

The split spectrum method is an alternative way (Schiestel, 1987) to derive de ε-equation in full statistical modeling for the case of homogeneous turbulence (fig. 1). A splitting wavenumber κ_d is defined by :

$$\kappa_d = \xi_d \frac{\varepsilon}{k^{3/2}} \qquad (4)$$

where k is the turbulence kinetic energy and ξ_d a numerical constant chosen such that κ_d is located in the higher range after the transfer zone. If $\mathcal{F}_d$ denotes the local energy flux at this wavenumber and F_d the net energy transfer, we then have :

$$F_d = \mathcal{F}_d - \mathcal{E}_d \frac{d\,\kappa_d}{dt} \qquad (5)$$

where $\mathcal{E}_d$ is the corresponding value of the turbulence energy spectrum.

Using the approximation $F_d = \varepsilon$ deduced from the hypothesis that there is no appreciable energy at wavenumbers higher than κ_d, and taking into account the equation for turbulence kinetic energy :

$$\frac{dk}{dt} = P - \varepsilon \qquad (6)$$

where P denotes the production rate of energy. The transport equation for the dissipation rate can be derived from equations (4) and (5) :

$$\frac{d\varepsilon}{dt} = \underbrace{\frac{3}{2}}_{C_{\varepsilon 1}} \frac{\varepsilon P}{k} - \underbrace{\left[\frac{3}{2} - \frac{k}{\kappa_d \mathcal{E}_d}\left(\frac{\mathcal{F}_d}{\varepsilon} - 1\right)\right]}_{C_{\varepsilon 2}} \frac{\varepsilon^2}{k} \qquad (7)$$

where the $C_{\varepsilon 2}$ coefficient is dependent on the spectrum shape.

Subgrid scale modeling

In the case of LES, a cutoff κ_c is introduced in the medium range of eddies (fig. 2). The subgrid energy in the $[\kappa_c, \kappa_d]$ range is denoted k_s. The wavenumbers κ_c and κ_d are now chosen such that :

$$\kappa_d - \kappa_c = \xi \frac{\varepsilon}{k_s^{3/2}} \qquad (8)$$

where ξ depends on the spectrum shape and the previous method is modified as follows. The partial turbulence kinetic equation is written :

$$\frac{dk_s}{dt} = F_c - \varepsilon \qquad (9)$$

Using the relation $F_c = \mathcal{F}_c - \mathcal{E}_c \frac{d\,\kappa_c}{dt}$ together with (5) one can deduce from (8) :

$$\frac{d}{dt}\left(\xi \frac{\varepsilon}{k_s^{3/2}}\right) = \frac{\mathcal{F}_d - \varepsilon}{\mathcal{E}_d} - \frac{\mathcal{F}_c - F_c}{\mathcal{E}_c} \qquad (10)$$

The ε-equation is then derived from (9) and (10) with the hypotheses that $\mathcal{E}_d$ is much smaller than $\mathcal{E}_c$, that κ_d is much larger than κ_c and also that the grid size is fixed or slowly variable, implying thus $F_c \simeq \mathcal{F}_c$.

$$\frac{d\varepsilon}{dt} = \underbrace{\frac{3}{2}}_{C_{s1}} \frac{\varepsilon}{k_s} F_c - \underbrace{\left[\frac{3}{2} - \frac{k_s}{\kappa_d \mathcal{E}_d}\left(\frac{\mathcal{F}_d}{\varepsilon} - 1\right)\right]}_{C_{s2}} \frac{\varepsilon^2}{k_s} \qquad (11)$$

Comparing to equation (7), one readily finds :

$$C_{s1} = \frac{3}{2} \text{ and } C_{s2} = \frac{3}{2} + \frac{k_s}{k}\left(C_{\varepsilon 2} - \frac{3}{2}\right) \qquad (12)$$

where the coefficients C_{s1} and C_{s2} are no longer constants but function of the cutoff location.

Calibration

The particular case of the decay of turbulence behind a grid in the initial period of decay is considered for calibrating the model coefficients. It is usually admitted that the energy spectrum at very low wavenumbers behaves like $\mathcal{E} \approx C\,\kappa^{\mu}$ whereas

in the inertial range for larges values of κ, the Kolmogoroff spectrum has to be recovered. For convenience, we shall use a function that have the correct behaviour both at small wavenumbers and in the inertial range :

$$\mathcal{E}(\kappa) = \frac{\chi\,\varepsilon^{2/3}\,\kappa^{\mu}}{\left[\left(\chi\,\varepsilon^{2/3}C^{-1}\right)^{\frac{2}{5+3\mu}} + \kappa^{2/3}\right]^{\frac{5+3\mu}{2}}} \qquad (13)$$

where χ is the Kolmogorov constant ($\chi \approx 1.5$).

The hypothesis of permanence of big eddies is taken into account through the fact that C is supposed constant. Integration of the spectrum gives :

$$k = \frac{1}{\mu+1}\left(C^{\frac{2/3}{\mu+1}}\chi\varepsilon^{2/3}\right)^{3\left(\frac{\mu+1}{5+3\mu}\right)} \qquad (14)$$

It can be easily deduced from the previous equations that :

$$\frac{d\varepsilon}{dt} = -\underbrace{\left(\frac{3\mu+5}{2(\mu+1)}\right)}_{C_{\varepsilon 2}}.\frac{\varepsilon^2}{k} \qquad (15)$$

The usual value $C_{\varepsilon 2} = 1.92$ is obtained for $\mu = 1.4$ This decay law corresponds in fact to a self similar decay in which the spectrum varies in scale but not in shape. Defining a non-dimensional wavenumber $\eta = \kappa/\kappa_{ref}$, with $\kappa_{ref} = \varepsilon / k^{3/2}$, the energy spectrum is then $\mathcal{E}(\kappa) = k\,\mathcal{E}^*(\eta)/\kappa_{ref}$ with :

$$\mathcal{E}^*(\eta) = \chi\,\eta^{\mu}\left(\frac{\chi}{1+\mu} + \eta^{2/3}\right)^{-\frac{3\mu+5}{2}} \text{ and}$$

$$\mathcal{H}^*(\eta) = \int_0^{\eta} \mathcal{E}^* d\eta = \left(\frac{\chi\,\eta^{-2/3}}{1+\mu} + 1\right)^{-\frac{3}{2}(\mu+1)} \qquad (16)$$

The determination of the coefficient C_{s2} (12) can be made by evaluating the ratio k_s/k :

$$\frac{k_s}{k} = 1 - \mathcal{H}^*(\eta_c) \qquad (17)$$

The important feature of this approximation is that $k_s/k \approx 1.5\chi\eta_c^{-2/3}$ and $k_s/k \to 0$ when $\eta_c \to \infty$. So, in principle this analytic formula allows to specify the variations of the C_{s2} coefficient in the subgrid-scale ε-equation.

Practical formulation

In practice, we prefer to use a variant of scaling based on a dimensionless wave number $\mathcal{N}_c = \kappa_c\,\mathcal{L}$ where $\mathcal{L}$ is the characteristic length scale of the whole spectrum. The characteristic length scale $\mathcal{L}$ can be evaluated according to the Rotta definition $\mathcal{L} = \int_0^{\infty} (\mathcal{E}(\kappa)/\kappa).d\kappa$, but as long as wall flows are considered, the approximation $\mathcal{L} = K.z$ will be sufficient (z is the distance from the nearest wall and K=0.41). The cutoff wavenumber κ_c will be approximated by the filter width :

$$\kappa_c = \frac{1}{\Delta x.\Delta y.\Delta z} \qquad (18)$$

Instead of (17), we have used here a simplified function for k_s/k that retains the correct asymtotic behaviours. This empirical choice is :

$$C_{s1} = 1.5 \text{ and } C_{s2} = 1.5 + \frac{0.42}{1+\beta\mathcal{N}_c^{2/3}} \qquad (19)$$

We again emphasize the fact that the coefficient C_{s2} varies in compliance with the spatial step size. It is also interesting to remark that the difference $C_{s2} - C_{s1}$ varies from 0.42 for full statistical modeling down to zero when DNS is approached and is an indicator of the relative proportion of the spectrum which is modeled. In the limit of full statistical modeling, $k_s \to k$ and the usual k-ε model is exactly recovered with $C_{s1} = 1.50$ and $C_{s2} = 1.92$. In the limit of DNS, $k_s \to 0$ and $C_{s2} = C_{s1}$ and indeed the subgrid scale energy is not maintained.

The magnitude of the numerical coefficient β in (19) is chosen empirically by reference to the logarithmic boundary layer and to fully developed channel flow.

An order of magnitude of β can be obtained by reference to the logarithmic boundary layer in which $k \approx 4\,u_*^2$ and $\varepsilon = u_*^3/Ky$. Then, the previous relations imply $\eta_c = 4^{3/2}\mathcal{N}_c$ and therefore $\beta \approx 8/3\chi$, but considering the numerous approximations made, this parameter will be calibrated by trial and error on a plane channel flow calculation. In practice we have used β=2.5. Also, for the subgrid scale viscosity, in order to satisfy the necessary compatibility with the asymptotic k-ε full statistical model, we are led to choose :

$$\nu_{sgs} = C_{\mu}\frac{k_s^2}{\varepsilon} \text{ with } C_{\mu}=0.09 \qquad (20)$$

In non-homogeneous flows the turbulent diffusion terms have to be added into in the partial kinetic energy and dissipation equations using gradient diffusion hypothesis.

The final version of the model is then completed by low Reynolds number terms that are necessary to describe the near wall region. The extension is made by using a transposition of the k-ε model of Jones and Launder (1972).

NON-EQUILIBRIUM TURBULENCE : PERIODIC FORCING

Numerical calculations have been carried mainly on a coarse meshes (32x64x62 points) because it is the privileged field of application of the present approach. First of all, the fully developed turbulent channel flow has been used as a reference test case of a quasi-equilibrium turbulent flow. In this case, the transport model developed previously must give almost the same results that the well-known Smagorinsky model (with C_S=0.2 and viscous sublayer modification). It has been confirmed that, for mean quantities and turbulence levels, the two models give almost identical results that are in satisfactory agreement with measurements. An illustration is given on figure 3 for turbulence intensity.

Pulsed channel flow characteristics

To illustrate some of the potentials of the new model, the application to unsteady turbulent flow with periodic forcing is considered (Dejoan, 1998). Indeed, experimental results on pulsed channel flow (Binder et Kueny, 1981) exhibit important lag effects appearing between the modulation of the turbulent stresses and the mean axial velocity. The periodic forcing is produced by a longitudinal sinusoidal mean pressure gradient (fig. 4). The governing parameter (Tardu et al., 1994) for periodic wall flows is the dimensionless Stokes parameter defined by $l_s^+ = l_s\, u_*/\nu$ with $l_s = \sqrt{2\nu/\omega}$. The Stokes length l_s can be interpreted as the distance from the wall at which the oscillation is diffusing. Then, when the frequency is higher, the wall layer influenced by the oscillation becomes more and more confined near the wall, and much of the flow in the channel core is like a piston flow.

For $10. < l_s^+ < 13.$ (relaxation regime), important amplitude modulations of the turbulence are observed together with phase shift effects. We have chosen here $l_s^+ = 12.9$ expecting strong interaction between the imposed oscillation and the turbulence itself. The amplitude is chosen to be weak, the ratio $A_{\tilde{U}c} / U_C$ being of order of 5 per cent.

Like in the experiment, no appreciable effect is found on time mean values. However, if one examines phase-averaged quantities, important effects are observed.

Term decomposition

The analysis of unsteady periodic flows is based on a four-terms decomposition formalism :

$$q = \langle q \rangle + \tilde{q} + q'_{exp} + q'_{imp} \qquad (21)$$

The statistical mean value is identified to the phase average and it can be split into a time mean value and a periodic oscillation. The fluctuating turbulent part is composed of an explicit part which is simulated and an implicit part which is modeled.

In practice, statistical convergence is obtained after 24 periods in time for phase averaging.

Modulation of mean velocity

As far as amplitudes and phase shifts of the velocity are considered, the behaviour of the two-scale model is not very different from the Smagorinsky model and the results (fig. 5 and 6) are in satisfactory agreement with the experimental data of Binder and Kueny (1981), Tardu and Binder (1993) and Tardu et al. (1994). The results are not far from the Stokes solution showing a steep gradient at the wall. The same results are also presented for the velocity gradient (fig. 7 and 8) that is the driving mechanism for turbulence production. For both calculation, the $\partial \overline{U} / \partial z$ velocity gradient modulation induced by the forced oscillation is diffused across a distance of about $z^+ \approx 51.$ from the wall. The predicted near wall phase shift of the velocity gradient is sligthly smaller then the value corresponding to the Stokes solution. This may be explained by the parameter $l_s^+ = 12.9$ used in the simulation which is higher than the critical value $l_s^+ = 8.1$ given by Binder et al. (1981).

Modulation of the turbulence field

On the contrary, the effects observed on the Reynolds stresses are found to be strongly model dependent. In particular the phases lags given by the two models are very different. In all cases, the first Fourier mode for the oscillation of the turbulent Reynolds stresses has been found to be dominant.

The relative amplitude (with respect to the velocity oscillation amplitude) of the fundamental mode of the longitudinal turbulence intensity is given on figure 9 which shows a strong dependency on the model. The two measurements correspond to distinct experiments (with different amplitudes but the same value for l_s^+) give indeed different levels and the calculated values roughly fall inside the interval. This difference is not clear but the Smagorinsky model predictions seem to be too quickly damped away from the wall.

The phase shifts are correctly predicted by the split-spectrum two-equations model, whereas the

Smagorinsky model calculation produces appreciable discrepancies with the measurements (figure 10). The results are represented in terms of time delay which characterizes the diffusion speed of the modulation, by using the relation given by Tardu et al. (1994) with ϕ in radians :

$$\Delta t^+ = \frac{1}{2}\left(\phi_{u'\tilde{u}'} - \phi_{\tilde{U}c} \right) l_s^2 \qquad (22)$$

These experiments have shown that in the range $8.1 < l_s^+ < 34.$, the variations of the time delay versus distance from the wall, satisfy a linear law of decay such that $dz^+ / d(\Delta t^+) \approx 0.4$ for $z^+ > 30.$ The equivalent relation, recast in terms of phase lag, becomes $d\left(\phi_{u'\tilde{u}'} - \phi_{\tilde{U}c}\right) / dz^+ = 2.5\ \omega^+$ and is also found to be in good agreement with the split spectrum model predictions (fig. 10). Only the two-equation model has given a successful prediction of phase shifts by an account of time lag effects.

CONCLUDING REMARKS

The proposed subgrid scale transport model, based on spectral partitioning, introduces a new ε-equation in which the coefficients are functions of the cutoff location. The form of the equations is formally consistent with the extreme limits that are DNS and full statistical modeling. The proposed model is devised for LES with coarse grids and in particular in non-equilibrium flows such as unsteady flows. The method can be readily extended to more general models such as non-linear models.
The application to unsteady turbulent flows in pulsed channel has put in light some potentials of the method. More extended validation to a wide range of flows would be however desirable.

The calculations have been carried on the supercomputers at the IDRIS computer center in Paris which is gratefully acknowledged.

References

Binder G. , Kueny J.L., 1981, "Measurements of the periodic oscillations near the wall in unsteady turbulent channel flow", Unsteady Turbulent Shear Flows, IUTAM Symp. , Ed R. Michel, J. Cousteix, R. Houdeville, Springer, pp. 100-109.

Comte-Bellot G., 1965, "Ecoulement turbulent entre deux parois parallèles", *Publ. Scientifique et Technique du Ministère de l'Armée de l'Air*, n°419.

Deardorff J.W., 1973, "The use of subgrid transport equations in a three-dimensional model of atmospheric turbulence", *J. Fluid Engng. ASME*, vol. 95, pp. 429-438.

Dejoan A., 1998, "Simulation de grandes échelles turbulentes en écoulement de canal plan soumis à des perturbations instationnaires". Thèse de Doctorat Université d'Aix-Marseille II.

Feng M., Tardu S. and Binder G., 1993, "Inner region of unsteady channel flow", In *Near wall turbulent flows, ed. by R.M.C. So, C.G. Speziale & B.E. Launder*, New York, Elsevier.

Horiuti K. & Yoshizawa A., 1986, Large-eddy simulation of turbulent channel flow by 1-equation model, Notes on Numerical Fluid Mechanics, Vol. 15, *Ed. by U. Schumann and R. Friedrich*, Vieweg Verlag, pp. 119-134.

Hussain A.K.M.F. and Reynolds W.C., 1975, "Measurements in fully developed turbulent channel flow", *J. Fluids Engng. Trans. ASME I,* vol 97, pp. 568-578.

Jones W.P., Launder B.E., 1972, The prediction of laminarization with a two-equations model of turbulence, *Int. J. Heat Mass Transf*, vol. 15, p 301.

Kreplin H.P. and Eckelman H., 1979, "Behaviour of the three fluctuating velocity components in the wall region of a turbulent channel flow", *Phys. Fluids*, vol 22, n°7, pp.1233-1239.

Schiestel R., 1987, Multiple time scales modeling of turbulent flows in one point closures, *Phys. of Fluids,* vol. 30, n°3, pp. 722-731.

Schiestel R., Viazzo S., 1995, A Hermitian-Fourier numerical method for solving the incompressible Navier-Stokes equations, *Computers & Fluids*, vol. 24 , n°6, pp. 739-752.

Schumann U., 1975, "Subgrid scale model for finite difference simulations of turbulent flows in plane channels and annuli", *J. Comp. Phys.*, vol 18, pp. 367-404.

Tardu S. and Binder G., 1993, "Wall shear stress modulation in an unsteady turbulent channel flow with hight imposed frequencies", *Phys. Fluids, A*, vol 5(8), pp. 2028-2037.

Tardu S., Binder G., Blackwelder R., 1994, "Turbulent channel flow with large amplitude velocity oscillations", *J. Fluid Mech.*, vol. 267, pp. 109-151.

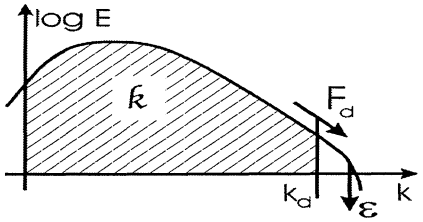

Figure 1 : Sketch of spectral integration for full statistical modeling.

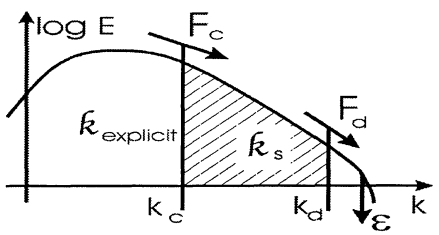

Figure 2 : Sketch of spectral partitioning for filtered turbulence.

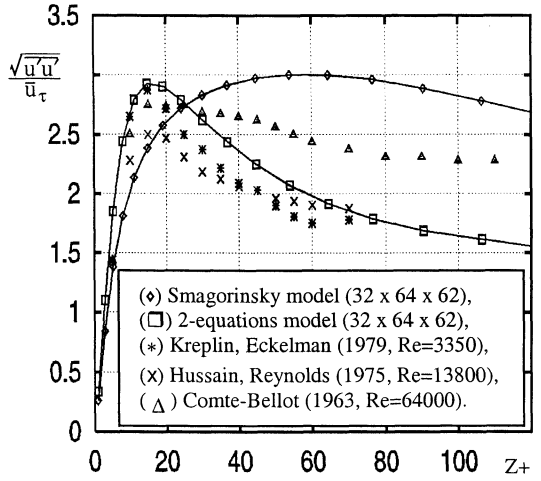

Figure 3 : Mean longitudinal turbulence intensity profiles in plane channel flow.

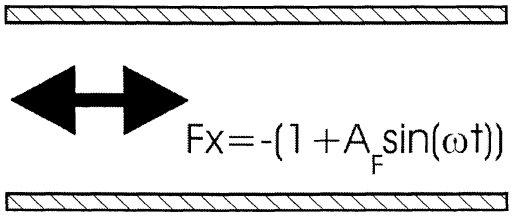

Figure 4 : Sketch of pulsed channel flow.

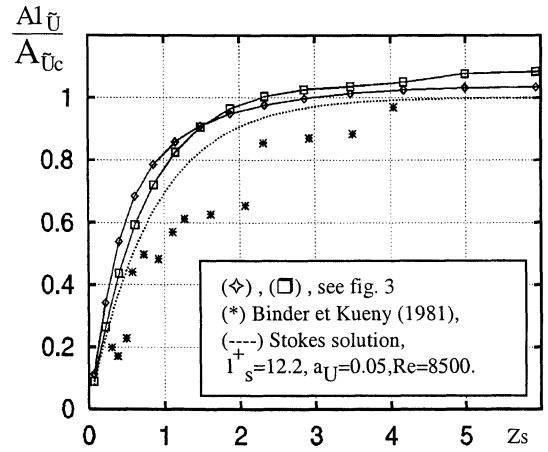

Figure 5 : Amplitude of the fundamental mode of the velocity modulation.

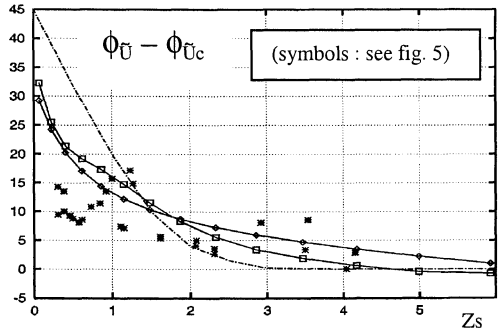

Figure 6 : Phase shift of the fundamental mode of the oscillating velocity deviation from axial velocity.

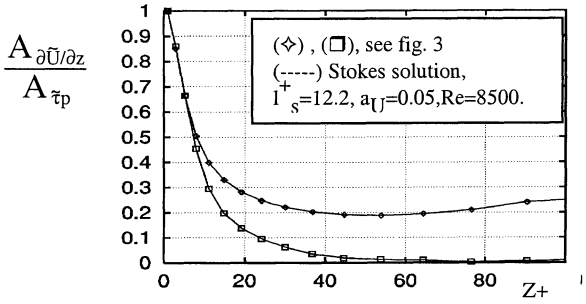

Figure 7 : Amplitude of the fundamental mode of the oscillating velocity gradient.

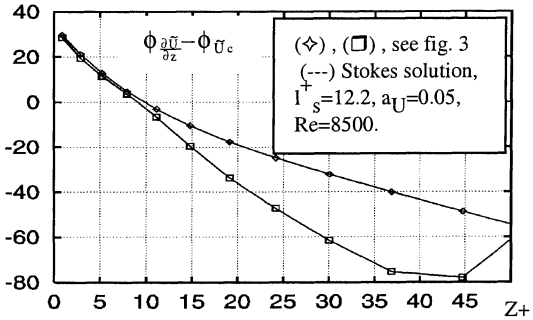

Figure 8 : Phase shift of the fundamental mode of the oscillating velocity gradient.

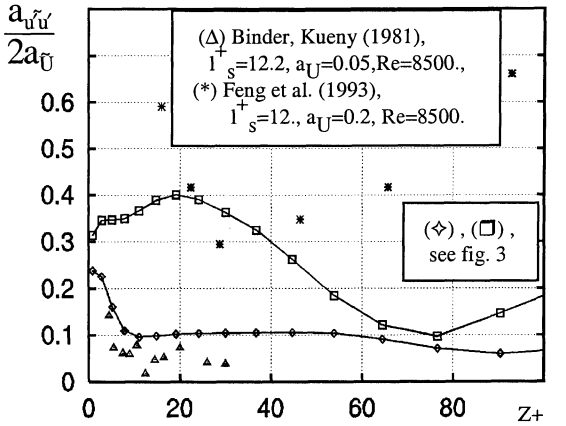

Figure 9 : Relative amplitude of the fundamental mode of the longitudinal turbulence intensity.

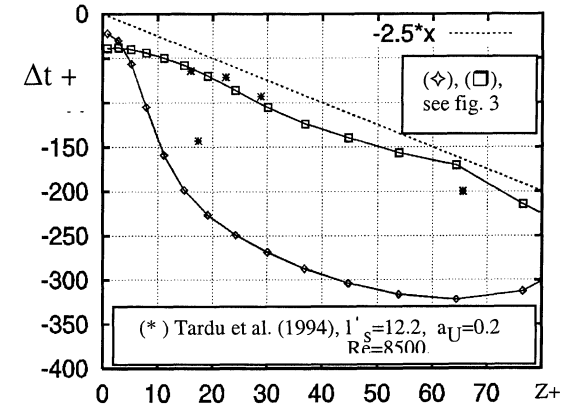

Figure 10 : Dimensionless diffusion time lag of the fundamental mode of the longitudinal turbulence intensity.